World Academy of Science, Engineering and Technology
International Journal of Mechanical and Mechatronics Engineering
Vol:8, No:1, 2014

Finite Element Analysis of Composite Frames in Wheelchair under Upward Loading

Thomas Jin-Chee Liu, Jin-Wei Liang, Wei-Long Chen, Teng-Hui Chen

***Abstract*—**The finite element analysis is adopted in this primary study. Using the Tsai-Wu criterion and delamination criterion, the stacking sequence $[45/0_4/-45_4/90_4]_s$ is the final optimal design for the wheelchair frame. On the contrary, the uni-directional laminates, i.e. $[90_{13}]_s$, $[45_{13}]_s$ and $[-45_{13}]_s$, are bad designs due to the higher failure indexes.

***Keywords*—**Wheelchair frame, stacking sequence, failure index, finite element.

I. Introduction

THE wheelchair frame is the main structure of the wheelchair for supporting the external loads and keeping the structural stiffness. The frame can be made stronger, but the weight needs to be limited. To improve the moving performance, the wheelchair weight has to be reduced. For this purpose, the light-weight materials can be adopted for making the wheelchair frame. However, the structural strength and stiffness also need to be kept. The best solution is to use the fiber-reinforced composite material due to its high strength-to-weight and stiffness-to-weight ratios.

The fiber-reinforced composite materials are composed of reinforced fibers and plastics matrix. They have unique advantages over monolithic materials, such as high strength, high stiffness, long fatigue life, low density, corrosion resistance, wear resistance and environmental stability [1]. The laminated fiber-reinforced composite materials such as carbon/epoxy or glass/polyester composites are widely applied in aircraft, aerospace, military, automotive, marine and sports structures [1], [2]. Using the carbon/epoxy composite materials, the wheelchair frame can reduce its weight effectively.

Solid mechanics is a powerful tool for the product design. With the aid of analytical or finite element calculations, the strength and stiffness of the wheelchair structures can be predicted or modified to obtain the optimal design. Using the finite element analysis, the design and structural behaviors of the wheel, frame and impact absorbing structure in the wheelchair have been studied [3]-[5]. However, there are few references to study the wheelchair frames associated with laminated composite materials in academic journals.

In [6], the fiber direction and stacking sequence design for the bicycle frame made of the carbon/epoxy composite laminates have been discussed by the finite element analysis. Using the maximum stress criterion and three testing methods, the stacking sequences $[0/90/90/0]_s$ and $[0/90/45/-45]_s$ are good designs for the composite bicycle frames. On the contrary, the uni-directional laminates, i.e. $[0/0/0/0]_s$, $[90/90/90/90]_s$, $[45/45/45/45]_s$ and $[-45/-45/-45/-45]_s$, are bad designs due to its higher stresses. The 0°-ply and 90°-ply located on the inner and outer layer of the tube can effectively resist the higher stress at its location [6].

Based on the research methodology established in [6], this paper will study and discuss the fiber direction and stacking sequence design for the wheelchair frames made of the carbon/epoxy composite laminates. The upward loading test is considered in this primary study. To predict the structure failure, the maximum stress criterion, Tsai-Wu criterion and delamination criterion are adopted. The failure index, i.e. stress-to-strength ratio, will be obtained to estimate the structural strength of the wheelchair frame. The finite element software ANSYS [7] will be employed to obtain the stresses and failure indexes.

II. Problem Definitions

A. Wheelchair Frame

In this study, the wheelchair frame system and its main dimensions are shown in Fig. 1. The wheelchair frame system consists of many tubular structures. All tubular frames are made of the carbon-fiber reinforced composite materials.

B. Composite Laminates

The composite materials of the wheelchair frames are the carbon-fiber reinforced (carbon/epoxy) composite laminates. As shown by different colors in Fig. 2, the tubular frames and connection regions are made of the 16-ply and 26-ply laminates, respectively. The connection regions use thicker structures (26-ply) to reduce the stress concentration. The thickness of each ply is 0.2mm.

Thomas Jin-Chee Liu, Associate Professor, is with the Department of Mechanical Engineering, Ming Chi University of Technology, Taishan, New Taipei City, Taiwan (corresponding author to provide phone: 886-2-29089899 ext 4569; e-mail: jinchee@mail.mcut.edu.tw).

Jin-Wei Liang, Professor, is with the Department of Mechanical Engineering, Ming Chi University of Technology, Taishan, New Taipei City, Taiwan.

Wei-Long Chen is a graduate student in the Graduate Institute of Electro-Mechanical Engineering, Ming Chi University of Technology, Taishan, New Taipei City, Taiwan.

Teng-Hui Chen, Assistant Professor, is with the Department of Mechanical Engineering, Yung Ta Institute of Technology & Commerce, Linlo, Pingtung County, Taiwan.

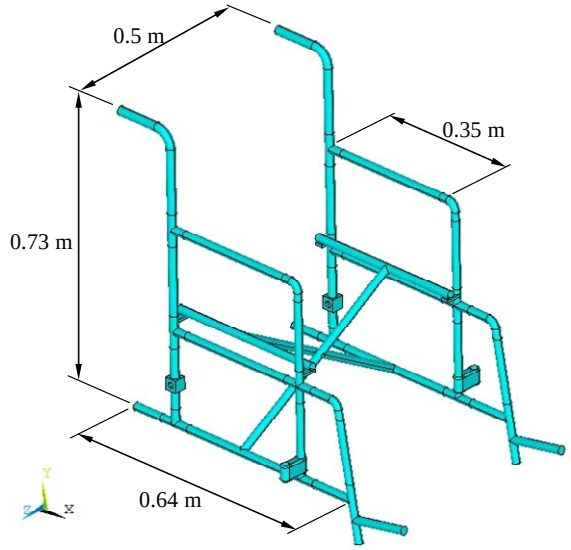

Fig. 1 Main dimensions of wheelchair frame system

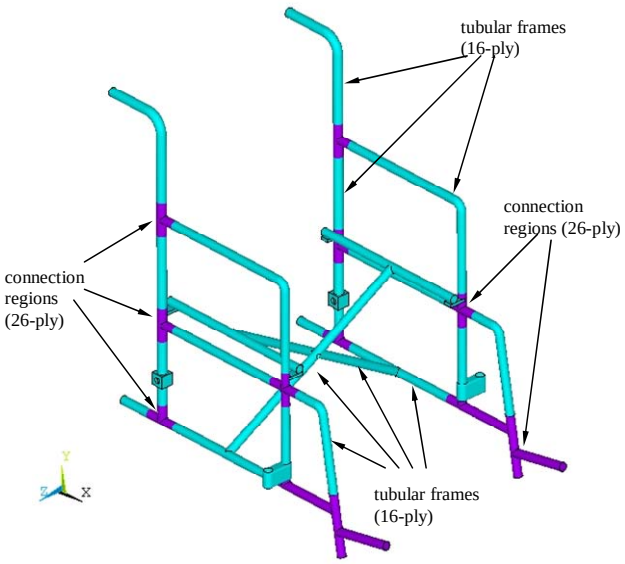

Fig. 2 Wheelchair frame system

Fig. 3 shows the symmetrical 26-ply laminate structure and the principal material coordinate system (PMCS) of each ply. In the 1-2-3 coordinate (PMCS), the 1-axis is prescribed as the fiber direction. The other coordinate *x-y-z* is the reference coordinate system (RCS) used to define the fiber angle. The fiber angle θ is defined as the angle between the 1-axis and *x*-axis. In this study, 16-ply and 26-ply symmetrical stacking sequences are denoted as $[(\theta_1)_2/(\theta_2)_2/(\theta_3)_2/(\theta_4)_2]_s$ and $[(\theta_1)/(\theta_2)_4/(\theta_3)_4/(\theta_4)_4]_s$, respectively.

In Table I, there are 33 stacking sequences of 26-ply laminates considered in this study. The stacking sequences in Table I are selected from four main fiber directions, i.e. θ = 0°, +45°, –45° and 90° which have been adopted in the past references for composite structures [6], [8]-[11]. The uni-directional laminates, i.e. Case 30 to 33 are analyzed for comparisons.

The stacking sequences of 16-ply laminates are similar to 26-ply. For example, the stacks $[0_2/90_2/45_2/-45_2]_s$ and $[0/90_4/45_4/-45_4]_s$ are simultaneously used in Case 1.

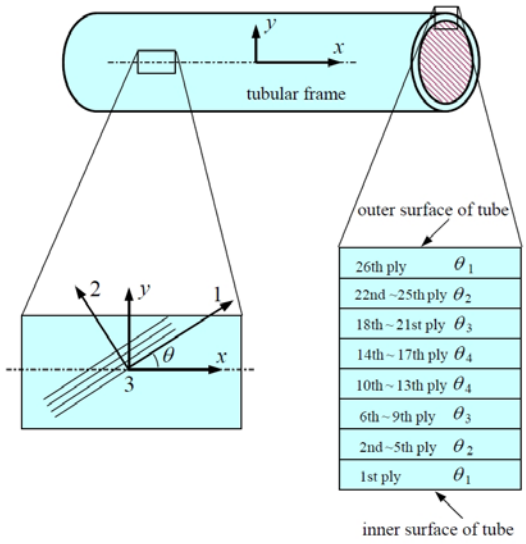

Fig. 3 26-ply laminated tubular frame

TABLE I
STACKING SEQUENCES OF 26-PLY LAMINATES IN THIS STUDY

Case	Stacking	Case	Stacking
1	$[0/90_4/45_4/-45_4]_s$	18	$[-45/45_4/90_4/0_4]_s$
2	$[0/45_4/90_4/-45_4]_s$	19	$[45/0_4/90_4/-45_4]_s$
3	$[0/-45_4/90_4/45_4]_s$	20	$[45/90_4/0_4/-45_4]_s$
4	$[0/90_4/-45_4/45_4]_s$	21	$[45/-45_4/0_4/90_4]_s$
5	$[0/45_4/-45_4/90_4]_s$	22	$[45/0_4/-45_4/90_4]_s$
6	$[0/-45_4/45_4/90_4]_s$	23	$[45/90_4/-45_4/0_4]_s$
7	$[90/45_4/-45_4/0_4]_s$	24	$[45/-45_4/90_4/0_4]_s$
8	$[90/-45_4/45_4/0_4]_s$	25	$[0/90_4/0_4/0_4]_s$
9	$[90/0_4/45_4/-45_4]_s$	26	$[0/0_4/90_4/0_4]_s$
10	$[90/45_4/0_4/-45_4]_s$	27	$[0/90_4/90_4/0_4]_s$
11	$[90/-45_4/0_4/45_4]_s$	28	$[90/0_4/0_4/90_4]_s$
12	$[90/0_4/-45_4/45_4]_s$	29	$[0/45_4/-45_4/0_4]_s$
13	$[-45/0_4/90_4/45_4]_s$	30	$[0_{13}]_s$
14	$[-45/90_4/0_4/45_4]_s$	31	$[90_{13}]_s$
15	$[-45/45_4/0_4/90_4]_s$	32	$[45_{13}]_s$
16	$[-45/0_4/45_4/90_4]_s$	33	$[-45_{13}]_s$
17	$[-45/90_4/45_4/0_4]_s$		

C. Testing Method for Wheelchair Frame

During the design process, the structural strength of the wheelchair frame needs to be verified by testing methods. Before creating real prototypes, the finite element models and computer simulations can be created to verify the structural behaviors. In this paper, the upward loading test is adopted [12]. Fig. 4 illustrates the loading and boundary conditions. Each handlebar is subjected to the force of 880 N.

To find the better composite stacking design, the stresses or failure indexes of each ply will be obtained from the finite element analyses. All analyses are assumed to be static and linear.

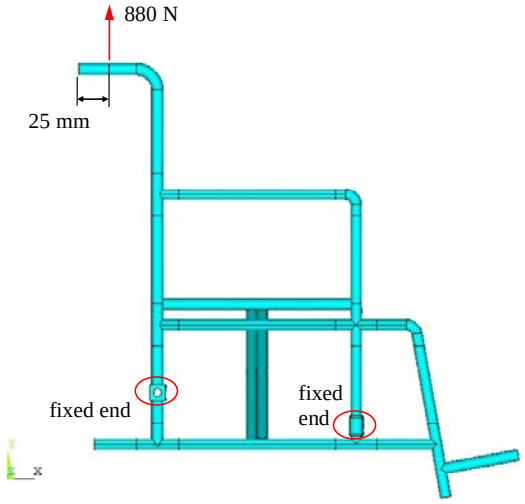

Fig. 4 Upward loading test

III. Methods of Analyses

A. Orthotropic Material Properties

Under the Cartesian coordinate 1-2-3 as shown in Fig. 3, the constitutive equation of the orthotropic material such as the carbon/epoxy composite is [1]:

$$\begin{bmatrix}\sigma_{11}\\ \sigma_{22}\\ \sigma_{33}\\ \tau_{23}\\ \tau_{31}\\ \tau_{12}\end{bmatrix}=\begin{bmatrix}C_{11} & C_{12} & C_{13} & 0 & 0 & 0\\ C_{21} & C_{22} & C_{23} & 0 & 0 & 0\\ C_{31} & C_{32} & C_{33} & 0 & 0 & 0\\ 0 & 0 & 0 & C_{44} & 0 & 0\\ 0 & 0 & 0 & 0 & C_{55} & 0\\ 0 & 0 & 0 & 0 & 0 & C_{66}\end{bmatrix}\begin{bmatrix}\varepsilon_{11}\\ \varepsilon_{22}\\ \varepsilon_{33}\\ \gamma_{23}\\ \gamma_{31}\\ \gamma_{12}\end{bmatrix} \quad (1)$$

Above equation can be written as a simple form:

$$\{\sigma\}=[C]\{\varepsilon\} \quad (2)$$

where $\{\sigma\}$, $\{\varepsilon\}$ and $[C]$ are the stress, strain and stiffness matrix, respectively.

The compliance matrix $[S]$ is the inverse of $[C]$ as follows:

$$[S]=[C]^{-1}=\begin{bmatrix}\frac{1}{E_1} & \frac{-\nu_{21}}{E_2} & \frac{-\nu_{31}}{E_3} & 0 & 0 & 0\\ \frac{-\nu_{12}}{E_1} & \frac{1}{E_2} & \frac{-\nu_{32}}{E_3} & 0 & 0 & 0\\ \frac{-\nu_{13}}{E_1} & \frac{-\nu_{23}}{E_2} & \frac{1}{E_3} & 0 & 0 & 0\\ 0 & 0 & 0 & \frac{1}{G_{23}} & 0 & 0\\ 0 & 0 & 0 & 0 & \frac{1}{G_{31}} & 0\\ 0 & 0 & 0 & 0 & 0 & \frac{1}{G_{12}}\end{bmatrix} \quad (3)$$

where E_i, G_{ij} and ν_{ij} are the Young's modulus, shear modulus and Poisson's ratio, respectively. The symmetrical matrix $[S]$ in (3) has nine independent material constants for the orthotropic material.

In the carbon/epoxy composite laminate, each ply has the orthotropic material property. The fiber directions of each ply can be different for practical applications. Table II lists the material constants of the carbon/epoxy composite material [11]. In this table, the subscript 1 denotes the fiber axis. In Fig. 3, the Cartesian coordinate 1-2-3 is considered as the PMCS of each ply. Nine material constants in Table II will be used in the finite element analyses. It is noted that the composite material property in Table II has the transverse isotropy with the 2-3 plane as the plane of isotropy.

TABLE II
Material Constants of Carbon/Epoxy Composite [11]
(The Subscript 1 Is the Fiber Axis)

Young's modulus (GPa)		
E_1	E_2	E_3
162	14.9	14.9
Poisson's ratio		
ν_{12}	ν_{13}	ν_{23}
0.283	0.283	0.386
Shear modulus (GPa)		
G_{12}	G_{13}	G_{23}
5.7	5.7	5.4

B. Maximum Stress Failure Criterion

The maximum stress failure criterion [1] is one of the failure criteria adopted in this study. The failure occurs when at least one stress component along one axis of the PMCS exceeds the corresponding strength in that direction [1]. Considering the stresses σ_1, σ_2, σ_3, τ_{23}, τ_{31} and τ_{12} based on the PMCS in Fig. 3, the maximum stress criterion is expressed as follows [1]:

$$\sigma_1=\begin{cases}S_{1t} & \text{when} \quad \sigma_1>0\\ -S_{1c} & \text{when} \quad \sigma_1<0\end{cases} \quad (4)$$

$$\sigma_2=\begin{cases}S_{2t} & \text{when} \quad \sigma_2>0\\ -S_{2c} & \text{when} \quad \sigma_2<0\end{cases} \quad (5)$$

$$\sigma_3=\begin{cases}S_{3t} & \text{when} \quad \sigma_3>0\\ -S_{3c} & \text{when} \quad \sigma_3<0\end{cases} \quad (6)$$

$$|\tau_{23}|=S_{23} \quad (7)$$

$$|\tau_{31}|=S_{31} \quad (8)$$

$$|\tau_{12}|=S_{12} \quad (9)$$

where S_{it}, S_{ic} and S_{ij} (i,j = 1,2,3) are the tensile, compressive and shear strength values, respectively. The strength values of T300 carbon/epoxy composites in Table III [13], [14] are used in this study.

The failure index ξ_{MS} for the maximum stress criterion is defined as [15]:

$$\xi_{MS}=\max\left[\frac{\sigma_{it}}{S_{it}},\frac{|\sigma_{ic}|}{S_{ic}},\frac{|\tau_{ij}|}{S_{ij}}\right],\ i=1,2,3 \tag{10}$$

where σ_{it} and σ_{ic} denote the tensile and compressive stress, respectively. When the failure index value is larger than 1, i.e. the stress value exceeds the strength value, the ply failure will occur.

TABLE III
STRENGTH VALUES OF CARBON/EPOXY COMPOSITE [13], [14]

Strength	Value (MPa)
S_{1t}	1760
S_{1c}	1570
S_{2t}	80
S_{2c}	246
S_{3t}	80
S_{3c}	246
S_{23}	98
S_{31}	98
S_{12}	98

C. Tsai-Wu Failure Criterion

The Tsai-Wu failure criterion [1], [16] is also adopted in this study. For the composite material which has the transverse isotropy with the 2-3 plane as the plane of isotropy, the Tsai-Wu criterion and its failure index ξ_{TW} are expressed as [1]:

$$\begin{aligned}&f_1\sigma_1+f_2(\sigma_2+\sigma_3)+f_{11}\sigma_1^2+f_{22}(\sigma_2^2+\sigma_3^2)+f_{44}\tau_{23}^2\\&+f_{66}(\tau_{31}^2+\tau_{12}^2)+2f_{12}(\sigma_1\sigma_2+\sigma_1\sigma_3)+2f_{23}\sigma_2\sigma_3=\xi_{TW}\end{aligned} \tag{11}$$

where f is the strength coefficient as follows [1]:

$$\begin{aligned}f_1&=\frac{1}{S_{1t}}-\frac{1}{S_{1c}},\quad f_2=\frac{1}{S_{2t}}-\frac{1}{S_{2c}},\\f_{11}&=\frac{1}{S_{1t}S_{1c}},\quad f_{22}=\frac{1}{S_{2t}S_{2c}},\\f_{44}&=\frac{1}{S_{23}^2},\quad f_{66}=\frac{1}{S_{12}^2},\\f_{12}&\cong\frac{-1}{2}\sqrt{f_{11}f_{22}},\quad f_{23}=\frac{1}{S_{2t}S_{2c}}-\frac{1}{2S_{23}^2}\end{aligned} \tag{12}$$

When ξ_{TW} > 1, the ply failure will occur.

D. Delamination Failure Criterion

In addition to the failure in each ply, the delamination failure between two plies is also considered. Using the interlaminar shear stress, the delamination failure criterion is assumed as follows:

$$\xi_D=\max\left[\frac{|\tau_{\text{int}13}|}{S_{\text{int}}},\frac{|\tau_{\text{int}23}|}{S_{\text{int}}}\right] \tag{13}$$

where τ_{int13} and τ_{int23} denote the interlaminar shear stresses on the interlaminar plane. S_{int} is the interlaminar shear strength. For T300 carbon/epoxy composite laminate, S_{int} is 96.5 MPa [17]. When ξ_D > 1, the delamination failure will occur.

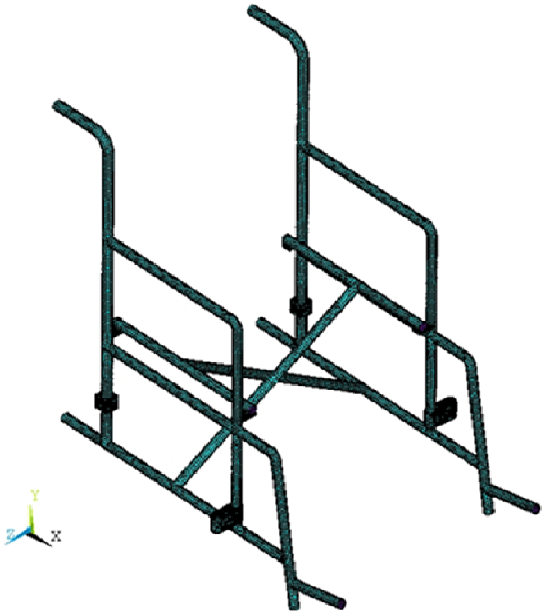

Fig. 5 Finite element model

E. Finite Element Analysis

Figs. 5 to 7 show the finite element model of the wheelchair frames created by the software ANSYS [7]. Static structural analysis and linear elastic property are considered. The SHELL91 elements with multi-plies are used to simulate the carbon/epoxy composite laminates. SHELL91 is the 8-noded high-order shell element using the thick shell theory. In addition, the perfect bonding between plies is assumed in the finite element analysis.

The fiber directions of all plies can be changed to discuss its effects on the stress magnitude. The boundary conditions are prescribed on the specified nodes of the finite element model. The external loads on the frame are prescribed on many nodes.

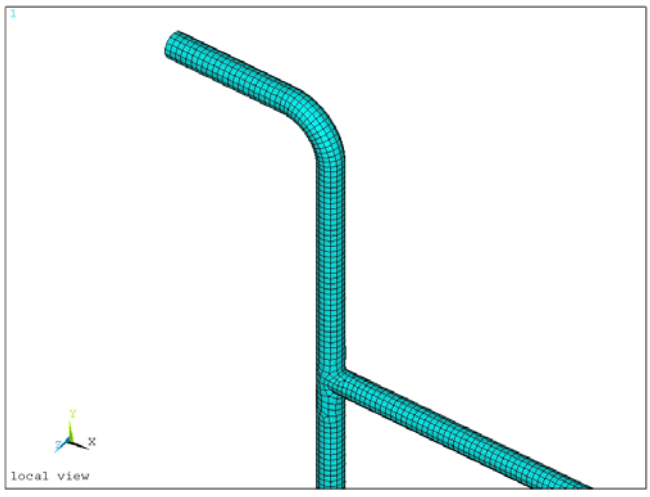

Fig. 6 Finite element model

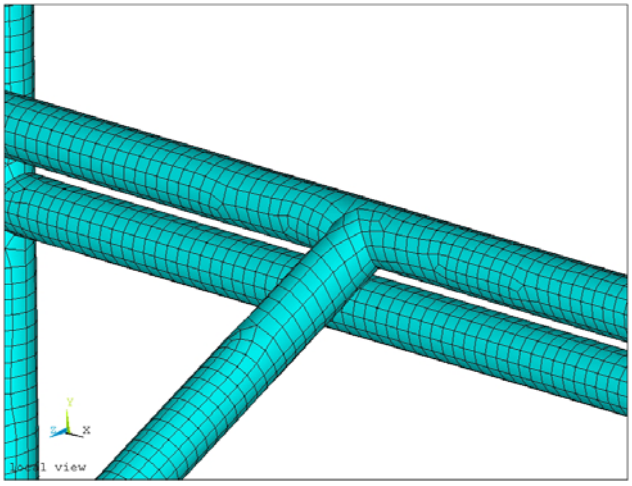

Fig. 7 Finite element model

F. Design Rule

All stacking sequences in Table I are used as the composite laminates of the wheelchair frame. Using the finite element analysis, the stresses of each stacking sequence are obtained under the upward loading. Then, the failure indexes ξ_{MS}, ξ_{TW} and ξ_{D} are calculated to estimate the structural performance.

The numerical results of connection regions (as shown in Fig. 2) are adopted for the structural design due to its local stress concentration. For each case in Table I, the stresses and failure indexes in all plies and on all interlaminar interfaces are obtained. Then, the maximum failure indexes ξ_{MSx}, ξ_{TWx} and ξ_{Dx} for each case are determined from those values. By comparing the values of ξ_{MSx}, ξ_{TWx} and ξ_{Dx} of 33 cases in Table I, the lowest value implies the optimal stacking sequence for the composite structure design.

IV. Results and Discussions

Figs. 8 to 10 show the variations of failure indexes ξ_{MSx}, ξ_{TWx} and ξ_{Dx} for 33 different stacking sequences. In these three figures, the cases which have lowest values are Case 12, 16 and 30, respectively. Based on the maximum stress criterion, Tsai-Wu criterion and delamination criterion, the optimal stacking sequences from three criteria are $[90/0_4/-45_4/45_4]_s$ (Case 12), $[-45/0_4/45_4/90_4]_s$ (Case 16) and $[0_{13}]_s$ (Case 30), respectively.

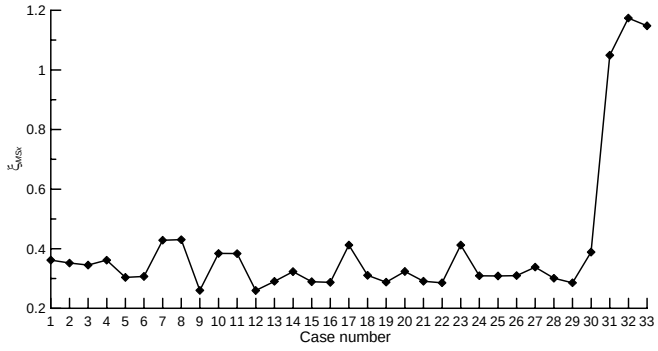

Fig. 8 Failure indexes ξ_{MSx} of different cases

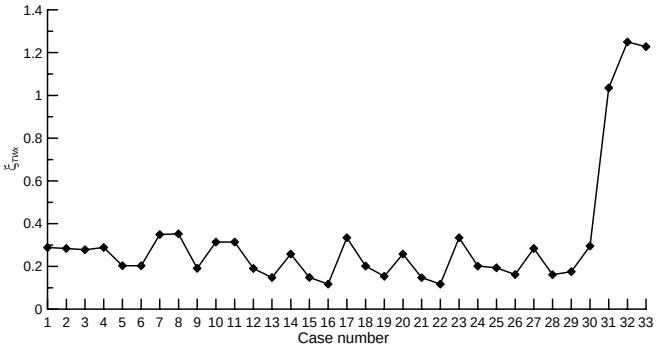

Fig. 9 Failure indexes ξ_{TWx} of different cases

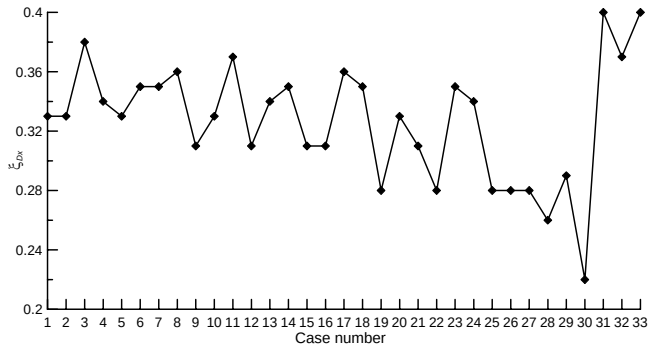

Fig. 10 Failure indexes ξ_{Dx} of different cases

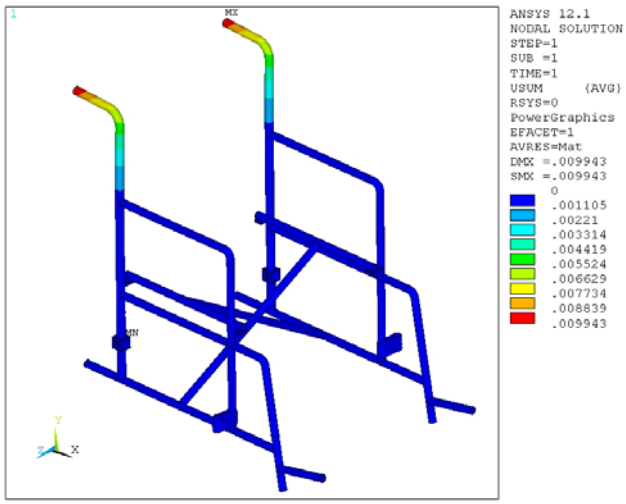

Fig. 11 Displacement contour of wheelchair frame system (Case 5) (units: m)

For the ply failure, the Tsai-Wu failure criterion is generally considered as the better rule. From this consideration, the stack $[-45/0_4/45_4/90_4]_s$ is the optimal design for the ply performance. However, the failure index ξ_{TWx} of another stack $[45/0_4/-45_4/90_4]_s$ (Case 22) is very near that of $[-45/0_4/45_4/90_4]_s$ (Case 16). The stacking sequence $[45/0_4/-45_4/90_4]_s$ can be considered as the second optimal design.

When the delamination criterion and Tsai-Wu criterion are simultaneously considered, the values of ξ_{Dx} of above two optimal designs need to be investigated. In Fig. 8, ξ_{Dx} of Case

22 is less than Case 16. To sum up, the stacking sequence $[45/0_4/-45_4/90_4]_s$ is the final optimal design. On the contrary, the uni-directional laminates, i.e. $[90_{13}]_s$, $[45_{13}]_s$ and $[-45_{13}]_s$, are bad designs due to the higher failure indexes as shown in Figs. 8 to 10. However, the stack $[0_{13}]_s$ (Case 30) is the optimal design according to the delamination criterion. Also, $[0_{13}]_s$ is not a bad design for Tsai-Wu criterion.

Fig. 11 shows the global deformation of the wheelchair frame system associated with $[0/45_4/-45_4/90_4]_s$ under the upward loading test. For the same case, Fig. 12 shows the distribution of the normal stress (σ_1) along the fiber direction on the outer surface of the tubular frame. The stress concentration can be seen around the connection region.

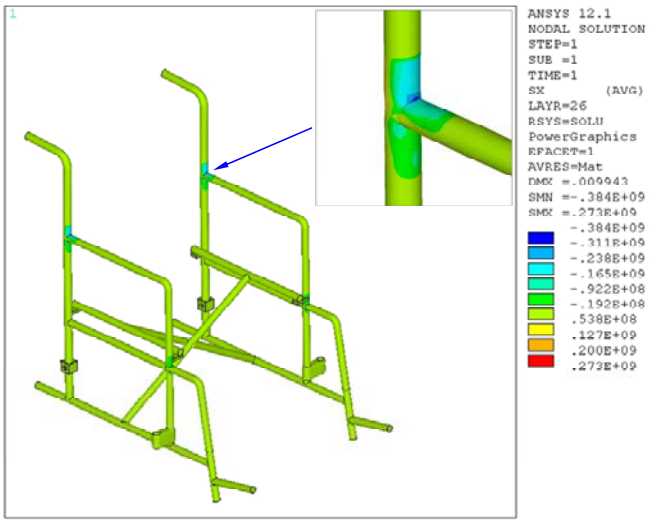

Fig. 12 Contour of normal stress (σ_1) along fiber direction on outer surface (Case 5) (units: Pa)

V. Conclusions

In this primary study, the fiber direction and stacking sequence design have been discussed for the wheelchair frames made of the carbon/epoxy composite laminates. Under the upward loading test, the finite element results are obtained. Using the Tsai-Wu criterion and delamination criterion, the stacking sequence $[45/0_4/-45_4/90_4]_s$ is the final optimal design. On the contrary, the uni-directional laminates, i.e. $[90_{13}]_s$, $[45_{13}]_s$ and $[-45_{13}]_s$, are bad designs due to the higher failure indexes.

Acknowledgments

The authors are grateful to the Ministry of Economic Affairs of R.O.C. Government in Taiwan for the financial support under contract number 101-EC-17-A-31-S1-207.

References

[1] Daniel IM, Ishai O. Engineering mechanics of composite materials. New York: Oxford University Press; 2006.
[2] Jones RM. Mechanics of composite materials. New York: McGraw-Hill; 1975.
[3] Kalyanasundaram S, Lowe A, Watters AJ. Finite element analysis and optimization of composite wheelchair wheels. Compos Struct 2006; 75: 393-399.
[4] MacLeish MS, Cooper RA, Harralson J, Ster III JF. Design of a composite monocoque frame racing wheelchair. J Rehabil Res Dev 1993; 30: 233-249.
[5] Yilmazcoban IK, Mimaroglu A. Frontal impact absorbing systems in wheelchairs like sheet metal hood in vehicles. Thin Wall Struct 2012; 59: 20-26.
[6] Liu TJC, Wu HC. Fiber direction and stacking sequence design for bicycle frame made of carbon/epoxy composite laminate. Mater Design 2010; 31: 1971-1980.
[7] ANSYS 12.1. USA : ANSYS, Inc.; 2009.
[8] Nelson R, Milovich D, Wilcox WM, Read RF. Composite bicycle frame and methods for its construction. US Patent, US 6270104 B1; 2001.
[9] Chue CH, Liu TJC. The effects of laminated composite patch with different stacking sequences on bonded repair. Compos Eng 1995; 5: 223-230.
[10] Lessard LB, Nemes JA, Lizotte PL. Utilization of FEA in the design of composite bicycle frames. Composites 1995; 26(1): 72-74.
[11] Liao CJ. Stiffness analysis of carbon fiber bicycle frame. Master thesis of Department of Mechanical and Computer Aided Engineering, Feng Chia University, Taiwan; 2007. (in Chinese)
[12] ISO 7176-8: 1998, Wheelchairs - Part 8: Requirements and test methods for static, impact, and fatigue strengths. Geneva: International Organization for Standardization; 1998.
[13] Torayca T300 data sheet. USA: Toray Carbon Fibers America, Inc.; 2009.
[14] Tsai SW, Hahn HT. Introduction to composite materials. US: Technomic Publishing; 1980.
[15] ANSYS 10.0 Documentation - ANSYS, Inc. Theory Reference. USA: SAS IP, Inc.; 2005.
[16] Tsai SW, Wu EM. A general theory of strength for anisotropic materials. J Compos Mater 5: 58-80; 1971.
[17] Mallick PK. Fiber-reinforced composites. Boca Raton: CRC Press; 2008.